ELSEVIER

Journal of Nuclear Materials 258–263 (1998) 74–84

journal of nuclear materials

Design and material selection for ITER first wall/blanket, divertor and vacuum vessel

K. Ioki *, V. Barabash, A. Cardella, F. Elio, Y. Gohar, G. Janeschitz, G. Johnson, G. Kalinin, D. Lousteau, M. Onozuka, R. Parker, G. Sannazzaro, R. Tivey

ITER JCT Garching, Boltzmannstraße 2, 85748 Garching, Germany

Abstract

Design and R&D have progressed on the ITER vacuum vessel, shielding and breeding blankets, and the divertor. The principal materials have been selected and the fabrication methods selected for most of the components based on design and R&D results. The resulting design changes are discussed for each system.

1. Vacuum vessel

The basic configuration of the vacuum vessel (VV) [1–3] has not changed during the last two years, however, important changes have been made in several areas to deal with natural convection cooling issues, increased loads due to asymmetric VDE's and the toroidal coil quench, additional neutron shielding requirements and the need to reduce toroidal field ripple.

The main vessel (Fig. 1) is a large double wall structure made from SS 316L(N)-IG (ITER Grade – 0.06–0.08% nitrogen). The outside diameter and height of the torus are 26 and 14.5 m, respectively. The inner and outer shells are made from 40 to 60 mm plate with stiffening ribs between them to give the vessel the required mechanical strength (Table 1). The total thickness of this structure is between 0.37 and 0.79 m. One of the major functions of the VV is neutron shielding. The space between the shells will be filled with plates made of a grade of SS 304 with 2% boron (UNS designation SS 30467). The addition of boron was recently adopted to improve neutron shielding efficiency. These plate "inserts" will fill ~60% of the volume between the vessel shells. A ferromagnetic material, SS 430, is used as the shielding material under the TF coils in the outboard area (12 o'clock to 3 o'clock) instead of SS 30467. These plates fill ~80% of the area between the shells and are estimated to reduce toroidal field ripple by a factor of 2.3 times from 1.6% to 0.7%. The toroidal resistance of the VV is 10.4 μΩ, while the total resistance of the VV plus Blanket is ~5 μΩ.

The ribs also form the flow passages for the forced vessel cooling/baking water to remove the 3 MW of nuclear heat deposition. The cooling water in the VV is routed to a manifold structure at the bottom of the sector and from here flows up both sides of the sector to the top and out. This basic arrangement of the VV, combined with the cooling system piping and the location of the heat exchanger, was selected to provide a system with maximum natural convection cooling during a loss of power or pump failure.

Increases in the peak loads imposed on the VV due to asymmetric VDE's and the toroidal coil quench have resulted in increases in the VV shell thickness to 60 mm in the inboard and lower areas of the vessel. For the case of an asymmetric VDE, the VV must support very high vertical and toroidal loads imposed by the blanket and divertor. Current estimates indicate that the total vertical load due to a category-III VDE event may be as high as 150 MN (12 MN maximum on an individual sector) and horizontal loads may be as high as 50 MN (5 MN maximum on an individual sector). These loads correspond to a halo current of 35% of plasma current and toroidal peaking factor of 1.65. The toroidal coil quench is expected to produce a pressure on the inner shell of ~2.2 MPa. The 60 mm shell thickness in these areas results in stresses within the allowable levels.

* Corresponding author. Tel.: +49 89 3299 4428; fax: +49 89 3299 4422; e-mail: iokik@sat.ipp-garching.mpg.de.

0022-3115/98/$19.00
PII: S0022-3115(98)00356-0

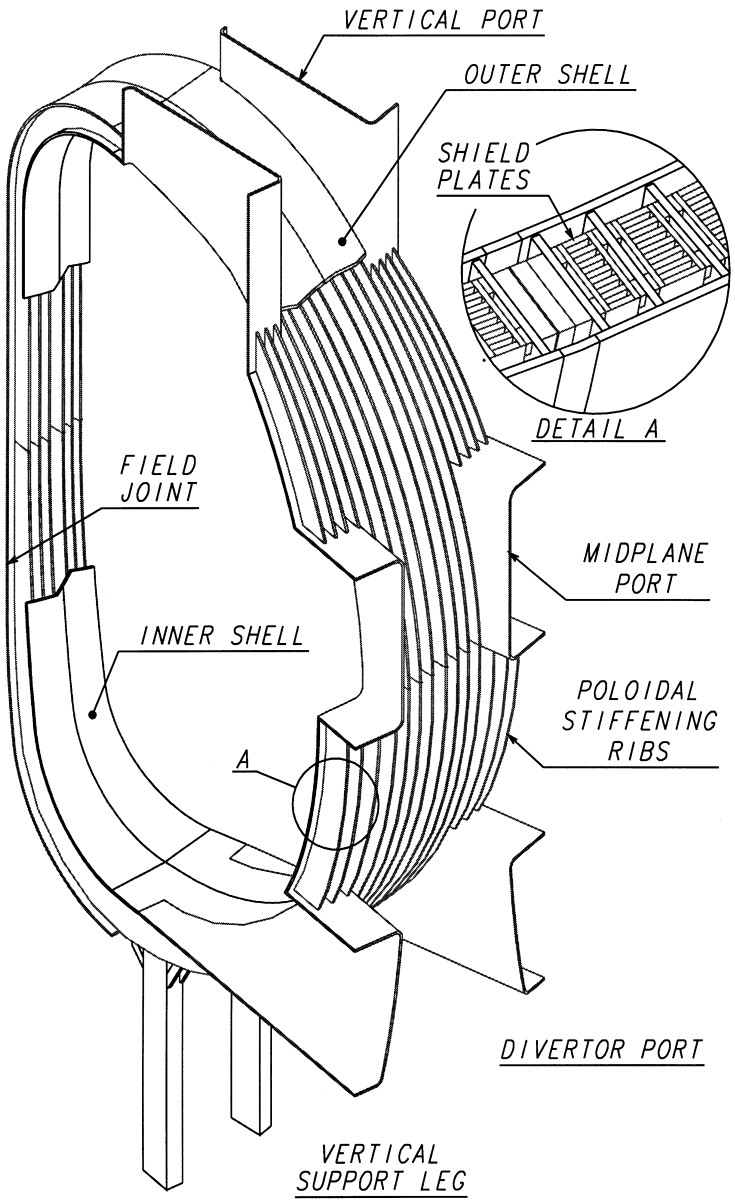

Fig. 1. Vacuum vessel sector.

The vessel has 20 vertical, 20 equatorial (17 regular and 3 NBI), and 20 divertor port structures. The vertical ports of the vacuum vessel are used as feed through points for the blanket cooling pipes (10 ports) and for viewing systems and diagnostics (10 ports). The blanket cooling pipes pass through the walls of the vertical ports and are routed to the blanket. The overall height of this port structure (~6 m) and the routing and design of the pipes enhance their flexibility and allow them to absorb the differential thermal expansion between the blanket and the VV, eliminating the need for bellows and increasing system reliability. The 10 vertical ports used for diagnostics are shorter (~3 m) and are used to mount many diagnostics including a neutron camera, a Thomson scattering diagnostic, and bolometry systems.

One of the most critical issues for the VV is the magnitude of welding distortions, dimensional accuracy and achievable tolerances. A single sector weighs ~270 t (without shielding) and may have as much as 20 t of weld material. How this amount of weld material would affect these parameters is being addressed by a full scale sector model which is the center piece of the VV R&D program. This model is being built as two 9° half sectors that are welded together to form the full sector. The fabrication

Table 1
Vacuum vessel parameters

Size	
Torus OD	26.2 m
Torus height	14.4 m
Double wall thickness	0.38–0.78 m
Toroidal extent of sector	18°
Shell thickness	40–60 mm
Rib thickness	30–60 mm
Weight	
Vessel and port structures (excl. shielding)	~5800 t
Shielding	~4000 t
Cooling	
Heat removal capacity	3 MW
Coolant fluid	Water
Total flow rate (normal op.)	80 kg/s
Total flow rate (fully developed natural convection)	~130 kg/s
Materials	
Main vessel	SS 316 L(N)-IG
Primary vessel shielding (with 2% boron)	SS 30467
Ferromagnetic shielding	SS 430

of these half sectors has been completed and a preliminary assessment of distortions and tolerances is consistent with expectations. Target tolerance values are ±5 mm for the sector height and ±6 mm for sector width. Hydraulic issues are being addressed by a 1/6 scale partial model of the VV cooling passages. The fabrication of the full scale sector model is complete and is providing key information required to finalize the VV design.

2. Blanket system

The Blanket System [4–6] (Fig. 2) for the Basic Performance Phase (BPP) is composed of blanket modules with a First Wall (FW) and shielding, and a support structure called a back plate (BP). The FW is subdivided into a primary wall, providing the first generic protection to the components behind it, the limiters that define the plasma boundary during plasma start-up and shutdown, and the baffles that have baffling function (Fig. 3). The primary and baffle modules mounted on the BP while the limiters are mounted in up to four equatorial ports.

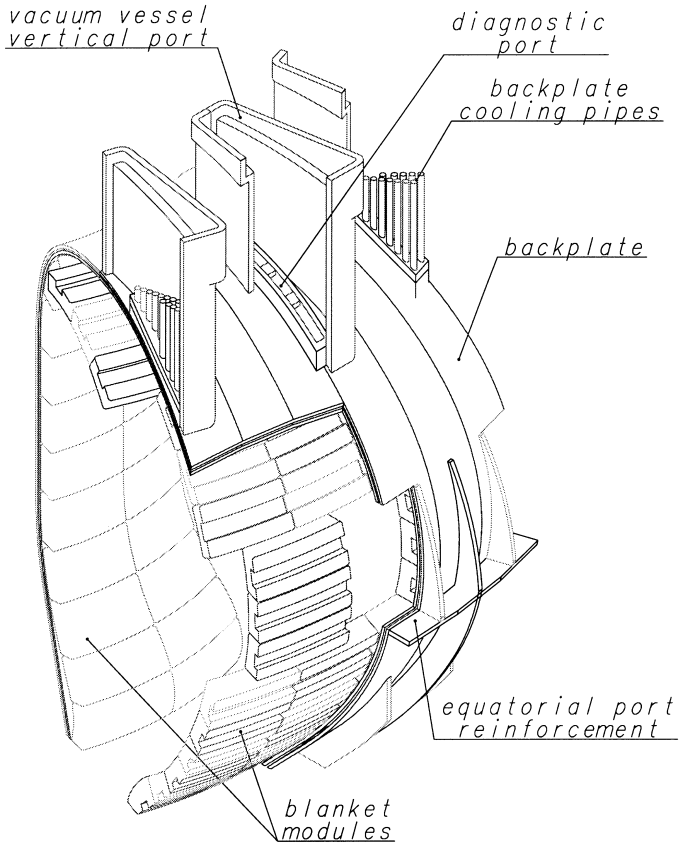

Fig. 2. Blanket system.

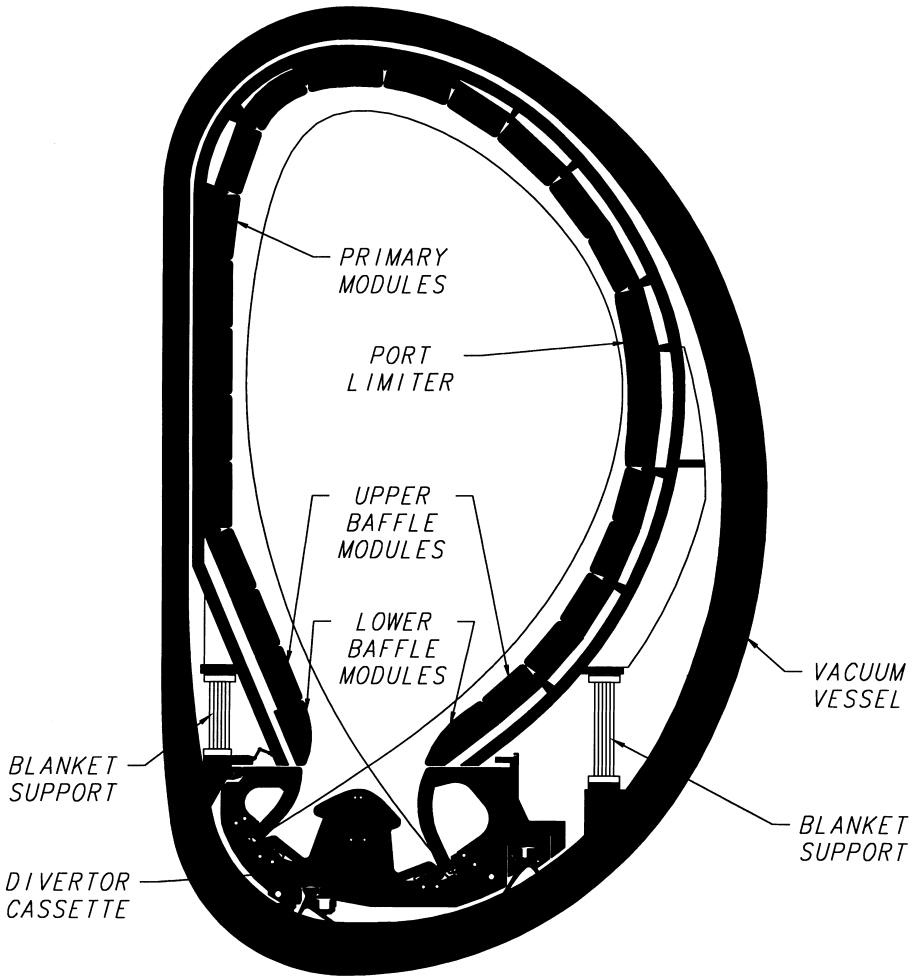

Fig. 3. Vertical cross-section of blanket system.

The BP is a toroidally continuous 316L(N)-IG stainless steel structure with a "horse-shoe" poloidal shape. It consists of two separated shells with an overall thickness of 160 mm (a 50 mm inner shell and a 70 mm outer shell). The 40 mm inter-space is used to channel the coolant water to the attached modules while cooling the BP itself. The water is supplied at 3.8 MPa and 140°C, with a temperature rise of ~50°C during normal operating conditions. The double wall structure was chosen to obtain higher mechanical strength with smaller distortion and better thermal response. It self-reacts all axisymmetric loads on the blanket while transmitting the net vertical and horizontal loads to the VV. The maximum electromagnetic pressure on the BP is ~4 MPa due to halo currents.

The FW/shield is composed of 739 modules. The segmentation was determined by the desire to minimize the number of module while meeting the weight limit of 4.3 t imposed by the remote maintenance equipment and the dimensions of the equatorial port. The module toroidal length varies from 1.5 to 2 m; the poloidal length, from 0.8 to 1.1 m.

Beryllium (S65CBe) is used as the plasma facing armour material at the primary FW, the limiter, and in the upper regions of the baffle because of its low atomic number, its ability to protect to the underlying FW structures from the off-normal thermal loads. It also offers lower retained tritium inventory when compared with CFC, and the prospect of in situ repair by plasma spray. The thickness of 10 mm is a compromise between maintaining reasonable maximum stress during normal operation and accommodating off-normal transient energy deposition (60 MJ/m^2 as maximum). W is used in the lower baffle near the divertor where the high particle flux which would cause excessive erosion rates on Be. The use of W also results in a considerable reduction of the tritium inventory.

The primary FW heat sink is made of an array of 10 mm diameter by 1 mm wall thick 316 L(N)-IG stainless steel tubes as shown in Fig. 4. The tubes are embedded in a copper alloy layer. A dispersion strengthened copper alloy Al25-IG is the first choice, with CuCrZr-IG as the back-up. Due to the higher heat fluxes, the baffle FW uses copper alloy tubes instead of tubes of stainless steel. A stainless steel liner, ~0.2 mm thick, will be used inside the copper tube to avoid corrosion problems. The shield section of the modules contains a coolant circuit in an arrangement of sets of parallel flow channels connected in series to the exit of FW tubes.

The module installation and replacement are performed from the plasma side. Each module has at least eight front access holes of 30 mm diameter each, four for the module attachments, two for the coolant connections, and two for the electrical connections. The attachment system (Fig. 5) is designed to transfer normal loads in the module to the BP while allowing small relative movement due to the different structural rigidities and thermal responses of the modules and the BP. A center pin establishes the module's position on the BP and reacts the net toroidal and poloidal loads. Alternating modules contain keys extending toroidally from both sides into key-ways in the adjacent modules to prevent rotation about the center pin. Each module also contains four radial supports shown in Fig. 6 that are designed to be flexible in the toroidal and poloidal direction. The flexible supports are made from Ti-alloy (Ti–6Al–4V) due to the compact design with its high strength and low Young's modulus. The supports are connected to the BP with Inconel 718 (ASTM B637) bolts. The preload 650 kN is adequately maintained under the nuclear heating and the stress cycle is within the fatigue limit.

Branch pipes provide the connection between the cooling circuits in the modules and those in the BP while upper and lower centrally located straps provide an electrical path for halo currents. The branch pipes and electrical straps are shown in Fig. 5. The branch pipe's end fittings will be from 316L(N) IG stainless steel and the pipe section from Inconel (Table 2). The electrical strap will be fabricated from CuCrZr alloy because of its low electrical resistance and relatively high strength at high temperatures. The center pin and flexible support connections include an electrical insulating break and the key way is electrically insulated from the remainder of the module so that adjacent modules are insulated. The branch pipes are not electrically insulated since the amount of current is acceptably small.

The limiters have been redesigned and moved to the ports for improved maintainability. As shown in Fig. 7, they are an assembly of 43 mm thick plates equal in length to the port height welded together at the rear section. Each plate is formed by HIPing two plates with an included cooling tube inserted into a serpentine path machined into both. The FW is added by HIPing the water cooled copper and ~4 mm thick Be layers to the plates. Swirl tapes enhance the performance of the FW cooling tubes.

The EB welded section forms a strong continuous assembly. The ~1 mm gap between plates is insulated with alumina to prevent arching. The vertical slots reduce the poloidal shear loads on the side walls by a factor of ~40. The ability of the plates to independently expand reduces the thermal stresses.

The centered disruption has been analyzed in two phases: a rapid thermal quench in 1 ms followed by a rapid current quench in 50 ms (changed from the previous time of 10 ms). Both toroidal and poloidal flux

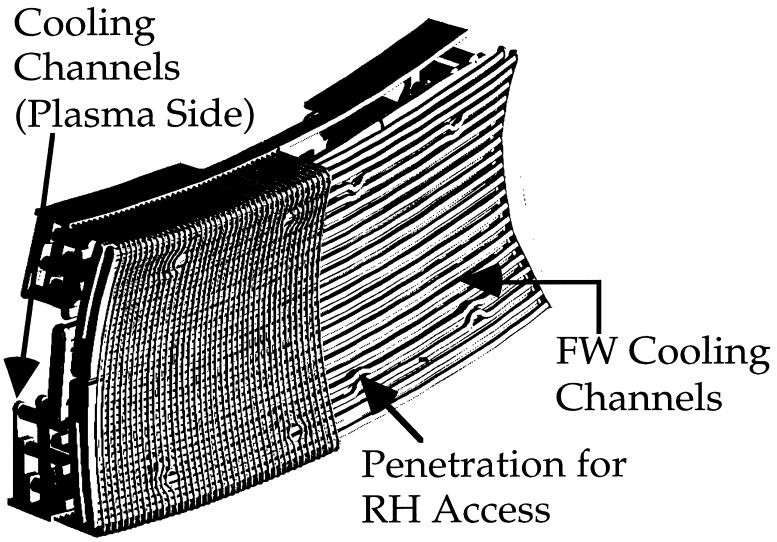

Fig. 4. FW and shield cooling layout.

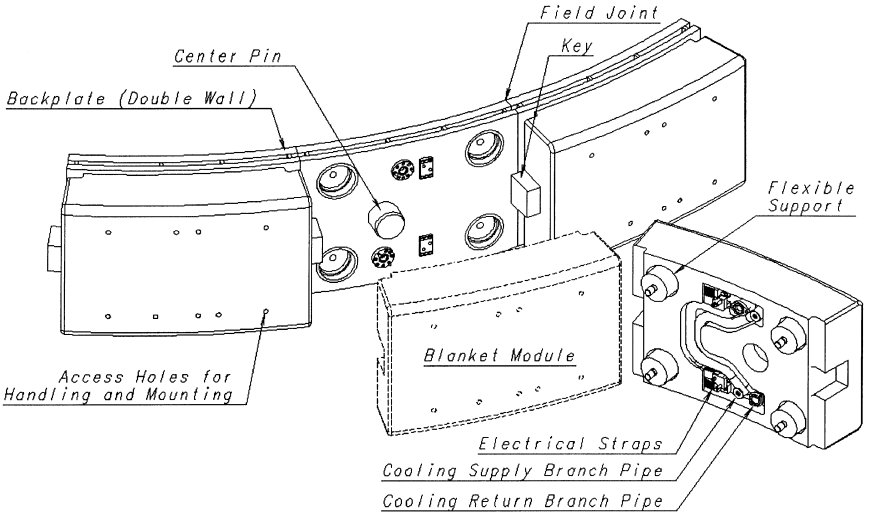

Fig. 5. Blanket module attachment.

change effect are now included in the modelling. The maximum poloidal current induced on the blanket is about 2.5 MA. The poloidal current interaction with the toroidal field produces the maximum pressure of about 0.7 MPa in the inboard midplane modules. The radial currents in a module produce a maximum load on the keys of ~0.9 MN, and the poloidal currents in a module produce a maximum load on the flexible supports of ~0.5 MN. In the VDE, a halo current of 7.35 MA (35% of initial plasma current) with a toroidal peaking factor of 1.65 enters the baffle modules in the inboard region, flows through the divertor structure, and goes out from the outboard baffle. The maximum halo current per module is 0.3 MA on the inboard baffle module with a

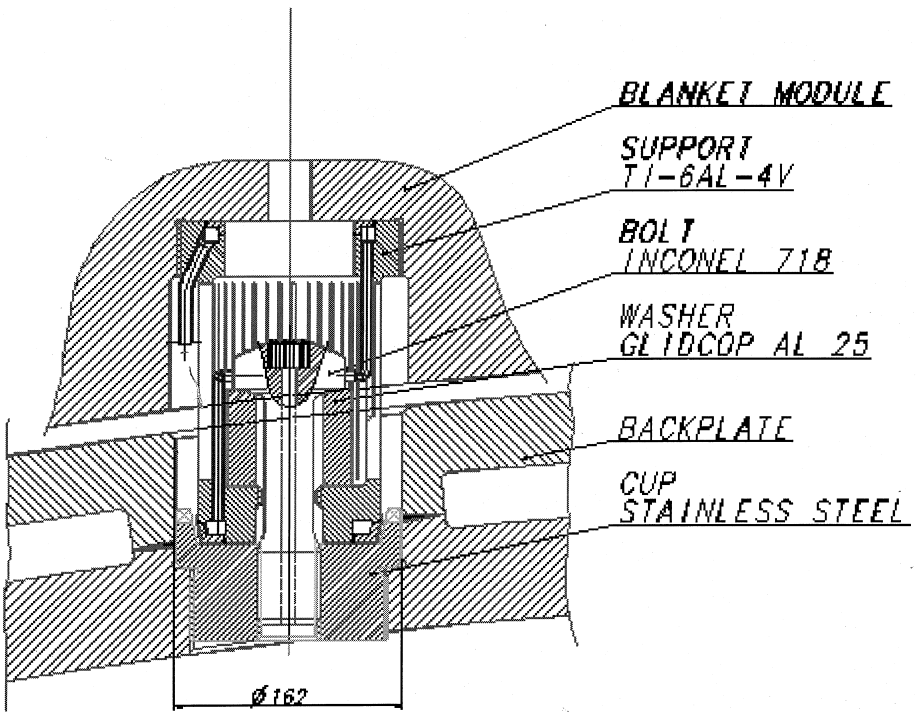

Fig. 6. Cross-section view of flexible support.

Table 2
Shield blanket parameters

Number of modules	
PW/Limiter/Baffle	459/160/120
First wall surface area	$\sim$ 1200 m^2
Weight	
Modules/Back plate/Total	2900/1450/4350 t
Material of module	
PFM-(PW)/(Limiter)/(Lower baffle)	BE/Be/W
Heat sink	Cu-Al25-IG
Coolant tube, shield block	316L(N)-IG
Coolant conditions type, pressure	Water, 3.8 Mpa
Inlet/Outlet temperature	140/190°C
Back plate	Double wall structure
Material	316L(N)-IG
Coolant velocity	$\sim$5 m/s
Attachment of modules	Flexible attachment
Material of flexible connector	Ti6Al4V
Key material	316L(N)-IG
Branch pipe	Flexible parallel pipes
Material	Inconel 625, 316L(N)-IG
Electrical strap	3-stage laminated
Material	CuCrZr-IG

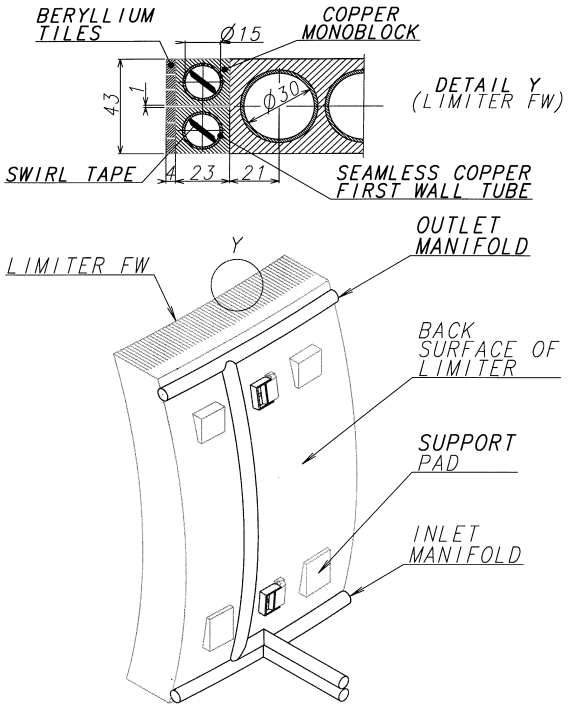

Fig. 7. Limiter in equatorial port.

halo current density on first wall is 0.18 MA/m^2. The maximum net force in poloidal direction is $\sim$1.0 MN on the inboard baffle which must be reacted by the module's center pin.

HIPing is the reference method for manufacture of the blanket modules due to the complex geometry and to the need to avoid welded or brazed joints near the plasma facing first wall. Solid HIPing has been chosen as the reference manufacturing technique since it has been shown to result in tight geometrical tolerance. The R&D program has produced and characterized copper to stainless steel joints in specimens by solid HIP, powder HIP, explosive bonding, and a combination of cold Isostatic pressing and HIP for a variety of copper alloys. The R&D program includes optimization of the HIP conditions (temperature, pressure, holding time) for single and multi-step HIPing, and development of UT NDE methods. Be–Cu alloy joints have been successfully made by HIP and brazing techniques and successfully tested under heat flux up to 12 MW/m^2, 4500 cycles. Joints of Be/Cu and Cu/SS have been irradiated in reactors and are presently being tested under heat loads. The R&D program has also produced data of the reweldability of irradiated SS and Inconel 625. Current activity is concentrating on producing mock-ups to demonstrate the module assembly with the mechanical attachment system. The demonstration of manufacturing techniques on full size prototypes of the FW/shield module and the BP is planned to be completed by 1999.

3. Breeding blanket

The breeding blanket [7] has the same modularity, installation, support, and replacement method. It uses a ceramic breeder for tritium breeding and water for heat removal with the same operating parameters as the shielding blanket. Lithium zirconate (Li_2ZrO_3) is the selected reference ceramic breeder because it has good irradiation stability, material compatibility with steel, low tritium inventory at low temperature, and low sensitivity to moisture. Its fabrication has been demonstrated by an industrial firm. Lithium titanate (Li_2TiO_3) is retained as an alternate breeder material because of its low activation. Enriched lithium is used to enhance the tritium breeding ratio. Both forms of Be material, block and pebbles, are under consideration for neutron multiplication. Block Be has high effective thermal conductivity relative to the pebbles that results in improved safety performance related to the water–Be interaction, and improved tritium breeding capability because of larger Be zone thickness without coolant panels. Be pebbles are used at the rear section to increase the operating temperature of the last breeder layer, where nuclear heating values are low. 316L(N)-IG stainless steel is used as structural material, see Table 3.

Table 3
Breeding blanket parameters

Plasma facing material	Beryllium
Structural material	316L(N)-SS
Breeder material	
Reference	Li_2ZrO_3
Alternative	Li_2TiO_3
Form	Pebbles
Li enrichment	90%
Min.–max. temperatures [a]	273–761
Tritium inventory	<100 g
Neutron multiplier	
Material	Beryllium
Form	Sintered Block and Pebbles
Sintered Min.–max. temp. [a]	167–344
Pebbles Min.–max. temp. [a]	181-412
Coolant	
Type	Water
Pressure	4 MPa
Inlet–outlet temperatures [a]	140–190°C
Tritium purge gas	
Gas	He + 0.1% H_2
Inlet pressure	~0.2 Mpa
Tritium breeding ratio	>0.8

[a] Temperatures during nominal operation.

Recently the breeding blanket module design was updated to incorporate the front access holes required for assembly.

The FW has a poloidal flow pattern with one coolant flow path to accommodate the toroidal surface heat flux during plasma disruption. Also, the breeding section has a poloidal coolant flow.

Most of the inboard blanket modules have two breeder zones embedded in Be with three coolant panels used to cool the module. The outboard blanket modules as well as some of the inboard blanket modules near the divertor zone are similar to the inboard except they have three breeder zones instead of two. This arrangement achieves a net tritium breeding ratio >0.8.

4. Divertor

The divertor [8–11] consists of 60 cassettes, each of which is approximately 2 m high, 5 m long and 0.5–1 m wide. Each cassette is mounted on inboard and outboard toroidal rails which are fixed to the vacuum vessel. The cassette body is a robust stainless steel structure cooled by water. The divertor cooling parameters are 140°C inlet temperature, 1 m^3/s flow rate in each of four separate circuits, 4 MPa inlet pressure, and 1.5 MPa pressure drop in-vessel through the divertor. Plasma facing components consist of a vertical target, a liner and a dome. Plasma facing components are mounted to the cassette body, and are demountable in a hot cell. The choice of the plasma facing materials has not changed. CFC is used in the lower region of the vertical target (VT) and the short dump target, and W is used in other regions where the heat flux is not exceeding 5 MW/m^2. The required lifetime of the plasma facing components is 3000 full power discharges as minimum.

A few design changes have been made in the divertor system. The dome is bigger to optimize neutral baffling. The attachment design of high heat flux components has been modified considering the remote maintainability. The dome body design has been modified to the modular plate structure similar to the VT. The heat load capability of the short dump target has been increased up to ~16 MW/m^2.

Operation with a semi-attached plasma has resulted in the development of a divertor without wings (Fig. 8). This option reduces the tritium codeposition and effectively cleans the tritium that is codeposited. In this design, surfaces in the private region are kept at high temperatures (450°C < T < 1200°C). The liner is clad with W set in a cast pure copper matrix, and subsequently EB welded to a CuCrZr heat sink (Fig. 9). Gas is exhausted through chevron shaped W armor blocks on stalks in the liner. Smooth surfaces allow local ECH discharges with oxygen gas, one of the most promising methods to remove codeposited tritium.

The cassette body has internal cooling channels which are optimized to reduce differential temperature and thermal stress due to nuclear heating and to withstand electromagnetic loads and internal water pressure. The cassette body is semi-permanent component which is expected to be used for the whole reactor life. The cassette body is made from SS 316 L(N)-IG by using cast/HIP or powder HIP method. As one of seven large R&D projects, a near full-scale mockup of the cassette body is now under construction by the home teams. The cast/HIP technology existing in aerospace industries has been improved and applied by the USHT.

The divertor is designed to exhaust 300 MW of surface heat load from a plasma plus approximately 100 MW of neutron bulk heating. The lower part of the VT has to accept almost all the power conducted in the SOL when the formation of a gas target fails or is delayed. The maximum heat flux reaches 20 MW/m^2 typically for 10 s, for up to 1000 events for the BPP. The heat loads during disruptions are ~100 MJ/m^2 in 0.1–3 ms and those during ELMs are ~10 MJ/m^2. In these off-normal conditions the CFC plasma facing surface will evaporate.

Vertical targets must be aligned accurately between adjacent cassettes in order to shield the leading edges from direct incidence of particles. The surface of the target plates is faceted, otherwise the peak heat flux at the edges becomes unacceptably high. A maximum step between adjacent targets of 4 mm provides peaking factors of 1.35 outboard and 1.4 inboard.

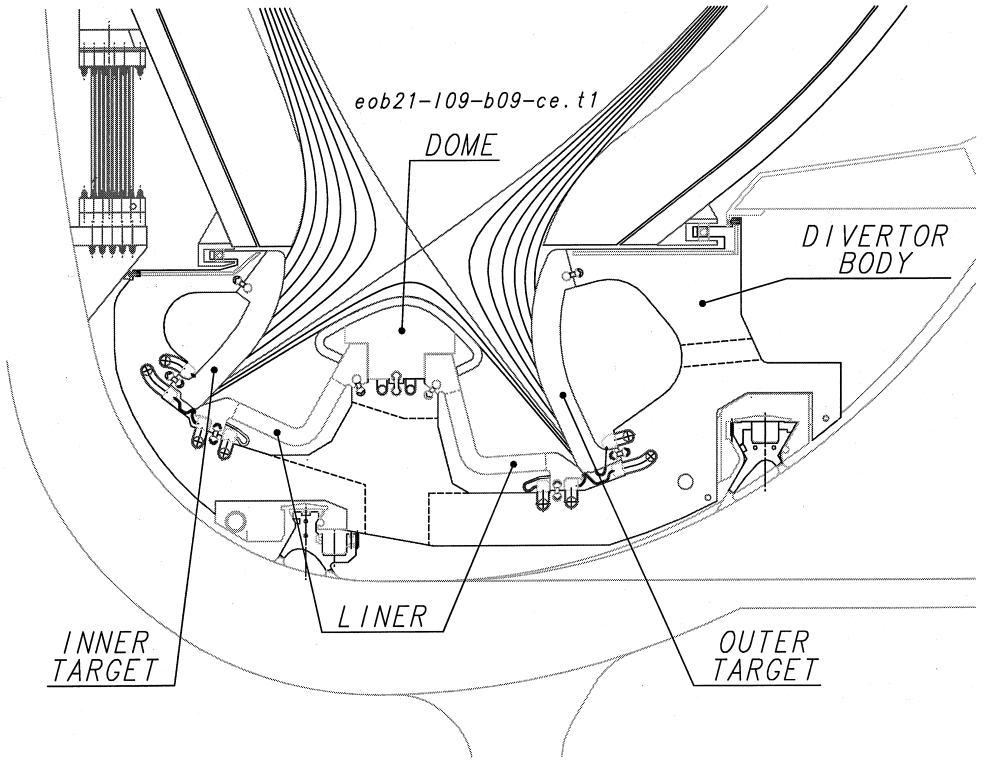

Fig. 8. Cross-section through divertor.

A CFC monoblock or saddleblock (Fig. 9) on a Cu tube will be used for the lower part of the VT and short dump targets. The primary bonding method between CFC and Cu is active metal casting or silver-free brazing. R&D fabrication and heat load tests of both approaches show encouraging results. CFC blocks and Cu heat sinks are attached to stainless steel plates with a thickness of ~50 mm. Thirteen plates in inboard and 18 plates in outboard are mechanically assembled together with long pins (Fig. 10). Swirl tubes with twist ratio ~2 are used to enhance the heat transfer coefficient and to realize higher CHF (Critical Heat Flux).

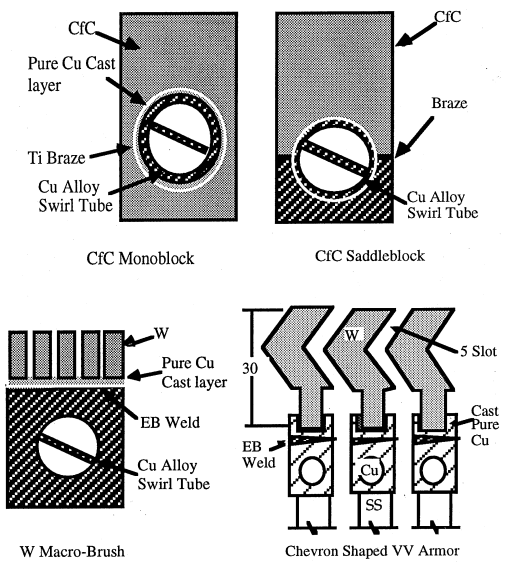

Fig. 9. Divertor plasma facing components.

4 × 4 mm × 10 mm thick W armor tiles (macrobrush) on Cu heat sinks are used for the upper part of the VT. The dome has also W armor tiles, and the heat sink Cu is mounted to stainless steel plates which are mounted to the cassette body. The primary W–Cu bonding method is active metal casting.

The main electromagnetic load in the divertor is due to halo currents during downward VDE's. The maximum halo current is ~0.2 MA/cassette, and the downward force is ~4.5 MN/cassette. The maximum EM load on the plasma facing components is ~4 MPa.

In R&D, fabrication and tests of PFC mock-ups have been done by the home teams. CFC monoblock and saddleblock mock-ups survived more than 1000 cycles of ~30 MW/m^2. W mockups fabricated by active metal casting survived ~1000 cycles of ~10 MW/m^2. The CHF tests have been done on swirl tubes and hypervapotron. CHF ~27 MW/m^2 was achieved in ITER-like conditions

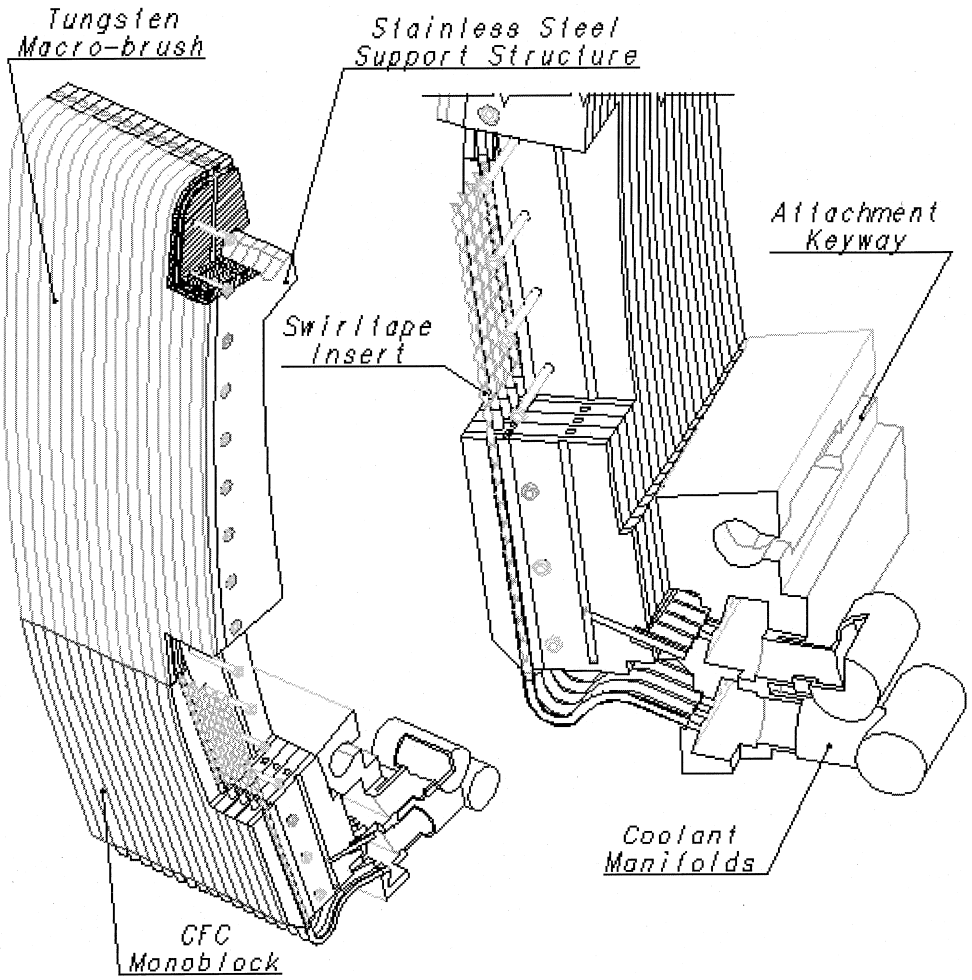

Fig. 10. Vertical target of divertor.

and heat flux profiles by the EUHT. Fabrication and tests of full scale mock-ups of the VT is now underway.

Acknowledgements

This report is an account of work undertaken within the framework of the ITER EDA Agreement. The views and opinions expressed herein do not necessarily reflect those of the partners to the ITER Agreement, the IAEA or any agency thereof. Dissemination of the information in this paper is governed by the applicable terms of the ITER EDA Agreement.

The authors wish to acknowledge the contributions of the other members of the Vacuum Vessel, Blanket, Divertor, and Materials Groups at the Garching Joint Work Site to the evolution of the design of the respective systems discussed in this paper. They also recognize the contributions in design and R&D of the members of the four Home Teams.

References

[1] K. Ioki et al., ITER vessel and blanket, in: Proceedings of the 16th IAEA Fusion Energy Conference, Montreal, October 1996, F1-CN-64/FP-7.
[2] K. Koizumi et al., Development of double-walled vacuum vessel for ITER, ibid., F1-CN-64/FP-8.
[3] M. Onozuka et al., Design progress of the vacuum vessel for ITER, in: Proceedings of the 17th Symposium on Fusion Engineering, San Diego, October 1997, to be published.
[4] K. Ioki et al., ITER blanket system design, in: Proceedings of the 19th Symposium on Fusion Technology, Lisbon, September 1996, p. 1331.
[5] K. Ioki et al., ITER first wall/shield blanket, in: Proceedings of the Fourth International Symposium on

Fusion Nuclear Technology, Tokyo, April 1997, to be published.
[6] W. Daenner et al., The ITER L-4 blanket project, in: Proceedings of the 16th IAEA Fusion Energy Conference, Montreal, October 1996, F1-CN-64/FP-9.
[7] Y. Gohar et al., ITER breeding blanket and demo relevant blanket test program, ibid., F1-CN-64/FP-10.
[8] M. Ulrickson et al., Development of a full-size divertor cassette prototype for ITER, ibid., F1-CN-64/FP-4.
[9] R. Tivey et al., Engineering design of the ITER divertor, in: Proceedings of 19th Symposium on Fusion Technology, Lisbon, September 1996, p. 279.
[10] G. Janeschitz et al., ITER physics basis, machine design and diagnostic integration in: Proceedings of the International Workshop on Diagnostics for Experimental Fusion Reactors, Varenna, September 1997, to be published.
[11] R. Matera, G. Federici, J. Nucl. Mater. 233 (1996) 17.